A VARIATION ON THE CHAMBERLIN TRIMETRIC MAP PROJECTION

B R S RECHT

Abstract. A variation of the Chamberlin Trimetric map projection is presented. This projection amounts to a linear transformation of the squares of the distances from a given point to three control points. It is significantly simpler to calculate than the Chamberlin projection, and allows for an inverse projection in the spherical approximation that only requires numerical estimation of one parameter. While it introduces slightly more distortion, the difference is small enough to be unnoticeable in most common use cases.

1. Introduction

[2][5][7]

2. Derivation of forward projection

This derivation will make heavy use of basic linear algebra: refer to a basic text on linear algebra, such as [8], if anything is unfamiliar.

Let $\mathbf{v}$ be a point on some ellipsoid, and let $\mathbf{p} = [x, y]$ be a point in the Euclidean plane. Let $d(\mathbf{v}_a, \mathbf{v}_b)$ be the geodesic distance between the points $\mathbf{v}_a$ and $\mathbf{v}_b$ on that ellipsoid. Let $\|\mathbf{p}\| = \sqrt{x^2 + y^2}$ be the Euclidean norm of the point $\mathbf{p}$, such that $\|\mathbf{p}_a - \mathbf{p}_b\|$ is the Euclidean distance between the points $\mathbf{p}_a$ and $\mathbf{p}_b$.

Let $\mathbf{v}_1$, $\mathbf{v}_2$, $\mathbf{v}_3$ be control points on the sphere, and $\mathbf{p}_1 = [x_1, y_1]$ etc. be the image of those control points on the plane, such that $d(\mathbf{v}_i, \mathbf{v}_j) = \|\mathbf{p}_i - \mathbf{p}_j\|$ for all i and j in $1, 2, 3$. The triangles with vertices at $\mathbf{v}_i$ or $\mathbf{p}_i$ will be called the control triangles (spherical or planar control triangle, respectively, if the distinction is important). Without loss of generality, also assume that $\|\mathbf{p}_i\|$ is the same for all i, such that the center of the circumcircle of the control triangle lies at the origin. (This just removes a translation in the plane in order to simplify the formula; false northing and easting can be added later.)

Let $r_i = d(\mathbf{v}_i, \mathbf{v})$ be the geodesic distance from $\mathbf{v}_i$ to $\mathbf{v}$, but also the radius of a circle that is centered at $\mathbf{v}_i$ and $\mathbf{v}$ lies on its boundary. The original Chamberlin projection draws a circle of radius r_i around each point $\mathbf{p}_i$, forming a small triangle with circular arcs for edges, and chooses a point $\mathbf{p}$ within that small triangle. Originally, in the 1950s when manual plotters were used, the exact definition of this point was not important, but Christensen [2] and most modern implementations (e.g. Proj [4]) use the centroid of the triangle formed by the points where each pair of circles intersect. Of course, each pair of circles intersects in (at most) two places, so the implementation must take care to choose the point of intersection that lies on the small triangle and not the other one.

One can make two observations on this configuration of circles in the plane. One is that the two points of intersection of each pair of circles are symmetric about the triangle edge between the two control points. The other is that, if one draws a line through the two points of intersection of each pair of circles, that line is perpendicular to the triangle edge, and once the lines are drawn for each pair of circles, the three lines appear to meet at the same point. (That observation will be proven true momentarily.) Although that point is not necessarily within the small triangle, it is for most points within the control triangle.

Suppose that $\mathbf{p}_1 = [-1, 0]$ and $\mathbf{p}_2 = [1, 0]$. Then the points of intersection of the circles with radius r_1 and r_2 are given as so:

$$\begin{aligned} x =& \frac{r_1^2 - r_2^2}{4} \\ y =& \pm \frac{1}{4}\sqrt{-\left(r_1 - r_2 - 2\right)\left(r_1 - r_2 + 2\right)\left(r_1 + r_2 - 2\right)\left(r_1 + r_2 + 2\right)} \end{aligned} \tag{1}$$

Date: January 2020.

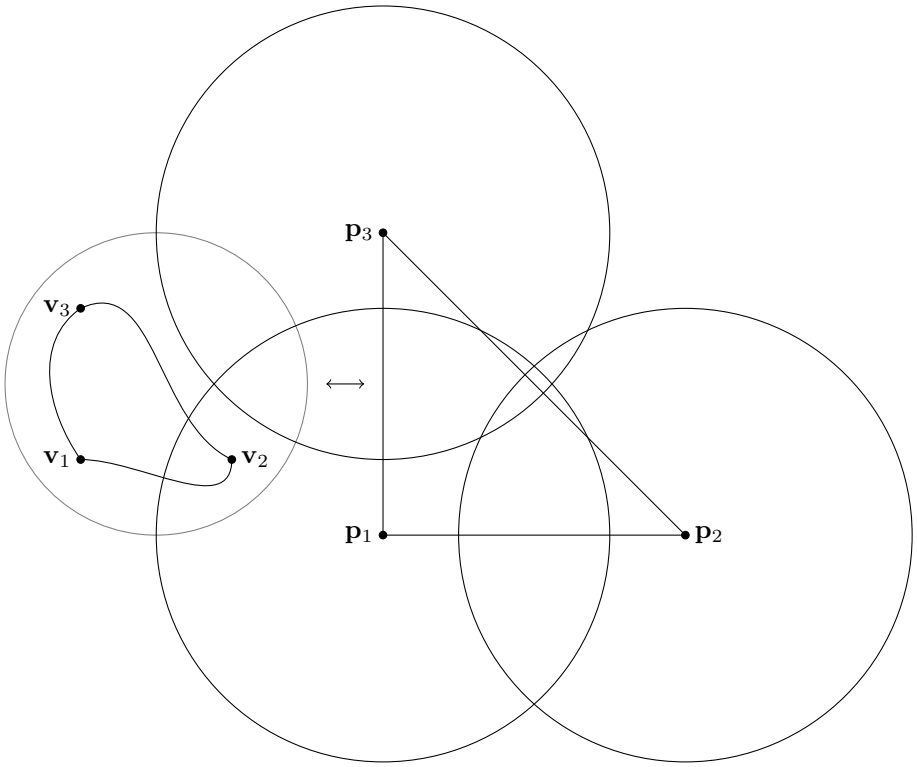

FIGURE 1. Depiction of Chamberlin projection.

Note that there is not necessarily a real solution for y. In that case, the circles do not intersect.

If a line passing through the two points of intersection is drawn, it intersects the triangle edge from $\mathbf{p}_1$ to $\mathbf{p}_2$ perpendicularly at the point with x as above and $y = 0$: call that point $\mathbf{p}_{12}$. In general form, one can use linear interpolation to determine the point of perpendicular intersection $\mathbf{p}_{ij}$ as so:

$$\mathbf{p}_{ij} = \mathbf{p}_i \frac{1 - t_{ij}}{2} + \mathbf{p}_j \frac{1 + t_{ij}}{2} \tag{2}$$

$$t_{ij} = \frac{r_i^2 - r_j^2}{\|\mathbf{p}_i - \mathbf{p}_j\|^2} \tag{3}$$

Note that this is defined for all r_i, regardless of whether the circles intersect.

The lines passing through $\mathbf{p}_{ij}$ and parallel to the line from p_i to p_j all meet at the same point. This can be proven with a simple triangle theorem sometimes attributed to Carnot: such lines meet at a single point if and only if [3][9]

$$\|\mathbf{p}_1 - \mathbf{p}_{12}\| + \|\mathbf{p}_2 - \mathbf{p}_{23}\| + \|\mathbf{p}_3 - \mathbf{p}_{31}\| = \|\mathbf{p}_2 - \mathbf{p}_{12}\| + \|\mathbf{p}_3 - \mathbf{p}_{23}\| + \|\mathbf{p}_1 - \mathbf{p}_{31}\| \tag{4}$$

for points $\mathbf{p}_{ij}$ lying on the edge between $\mathbf{p}_i$ and $\mathbf{p}_j$. Plugging in Equation 2 and simplifying proves that these lines satisfy this theorem.

The equation of the line passing from $\mathbf{p}_i$ to $\mathbf{p}_j$ is:

$$y(x_i - x_j) - x(y_i - y_j) - x_i y_j - x_j y_i = 0. \tag{5}$$

Thus, the equation of the line perpendicular to that line and passing through the point $\mathbf{p}_{ij}$ can be found to be

$$y(y_i - y_j) + x(x_i - x_j) + \frac{r_i^2 - r_j^2}{2} = 0. \tag{6}$$

Combining the equation of each perpendicular line creates a linear system. It is an overdetermined system of 3 equations in 2 variables, but since all 3 perpendicular lines meet at the same point as proven above, it has

a solution. Ultimately this system can be solved for $\mathbf{p}$ to define a map projection as follows. Let $\mathbf{P}$ be a 3x2 matrix having $\mathbf{p}_i$ as its ith column. Then:

$$\mathbf{p} = \mathbf{M} \begin{bmatrix} r_1^2 & r_2^2 & r_3^2 \end{bmatrix}^\top, \tag{7}$$

$$\mathbf{M} = \frac{1}{2T} \begin{bmatrix} y_3 - y_2 & y_1 - y_3 & y_2 - y_1 \\ x_2 - x_3 & x_3 - x_1 & x_1 - x_2 \end{bmatrix} = \frac{1}{2T} \begin{bmatrix} 0 & -1 \\ 1 & 0 \end{bmatrix} \mathbf{P} \begin{bmatrix} 0 & -1 & 1 \\ 1 & 0 & -1 \\ -1 & 1 & 0 \end{bmatrix}, \tag{8}$$

$$T = \begin{vmatrix} x_1 & x_2 & x_3 \\ y_1 & y_2 & y_3 \\ 1 & 1 & 1 \end{vmatrix}. \tag{9}$$

T is equal to twice the area of the Euclidean control triangle. T is zero if all the control points lie on a line, and is very small if the control points are very close to each other, in which case the matrix $\mathbf{M}$ is undefined or numerically unstable. (Of course, those are not typical use cases for the Chamberlin projection.)

The matrix $\mathbf{M}$ has a (right) nullspace spanned by the vector $[1, 1, 1]$. In general, this implies this projection is not one-to-one for all possible values of r_i: in particular, if $r_1 = r_2 = r_3$, then $\mathbf{p} = [0, 0]$. Of course, not all values of r_i correspond to actual points on the ellipsoid, but this projection will be observed later on to have overlap for some points outside the control triangle, much like the Chamberlin projection. (Again, the Chamberlin projection is not commonly used to project the entire earth, except for demonstration purposes.)

3. Inverse

Given $\mathbf{p}$, we start to invert the projection as so:

$$\begin{bmatrix} k_1 & k_2 & k_3 \end{bmatrix}^\top = \mathbf{M}^+ \mathbf{p}, \tag{10}$$

$$\mathbf{M}^+ = \frac{2}{3} \begin{bmatrix} 2x_1 - x_2 - x_3 & 2y_1 - y_2 - y_3 \\ -x_1 + 2x_2 - x_3 & -y_1 + 2y_2 - y_3 \\ -x_1 - x_2 + 2x_3 & -y_1 - y_2 + 2y_3 \end{bmatrix} = \frac{2}{3} \begin{bmatrix} -2 & 1 & 1 \\ 1 & -2 & 1 \\ 1 & 1 & -2 \end{bmatrix} \mathbf{P}^\top \tag{11}$$

$k_i = r_i^2 - h$ for some value h. This is a general solution to inverting Equation 7, thus the free parameter h. $\mathbf{M}^+$ is the pseudoinverse of $\mathbf{M}$ and vice versa. Because $\mathbf{M}^+$ has a left nullspace spanned by the vector $[1, 1, 1]$, it follows that $\sum_i k_i = 0$, which can be used to calculate k_i more efficiently.

By plugging Equation 7 into Equation 10, we can find that $h = \frac{1}{3} \sum_i r_i^2$. Unfortunately, if one attempts to solve for r_i given k_i, they find another general solution with one free parameter, putting them right back where they started. It turns out that information about the geoid needs to be introduced to determine r_i and $\mathbf{v}$. In the following, this is done with spherical approximation, and the case of an ellipsoid is discussed.

3.1. With spherical approximation.

If treating the earth as a unit sphere, then let $\mathbf{v} = [x, y, z]$ be a Euclidean vector such that its norm is 1: $\|\mathbf{v}\| = \sqrt{x^2 + y^2 + z^2} = 1$. In that case, spherical geometry allows an analytic way to determine a vector $\mathbf{v}$ given r_i. For this section, let r_i have units of radians of arc on the surface of the sphere. The circle of points $\mathbf{v}$ at distance r_0 from a point $\mathbf{v}_0$ is simply the circle where a plane intersects the sphere. This plane may be specified as so:

$$\mathbf{v}_0 \cdot \mathbf{v} = \cos(r_0). \tag{12}$$

Clearly, replacing $\mathbf{v}_0$ with $\mathbf{v}_i$ and r_0 with r_i for each i gives a linear system. Let $\mathbf{V}$ be the matrix having $\mathbf{v}_i$ as its ith column. Thus,

$$\mathbf{v} = \mathbf{V}^{-1} \begin{bmatrix} \cos(r_1) \\ \cos(r_2) \\ \cos(r_3) \end{bmatrix} \tag{13}$$

$\mathbf{V}^{-1}$ is undefined or numerically ill-behaved if the control points lie on a line or are very close together. It is also undefined if the points all lie on a great circle of the sphere: in that case, there are two points that satisfy the values of r_i. Again, those are not typical use cases for the Chamberlin projection.

FIGURE 2. Plot of $f(h)$ for a number of points.

FIGURE 3. Deviation after round-trip transformation. Units are kilometers.

For the point to lie on the unit sphere, $\|\mathbf{v}\| = 1$. Let $\mathbf{c}$ be a vector with ith component $\cos(r_i)$. Then,

$$\mathbf{c}^\top \left(\mathbf{V}^\top \mathbf{V}\right)^{-1} \mathbf{c} = 1 \tag{14}$$

Make the substitution $r_i = \sqrt{k_i + h}$. The result is a little opaque, but we now have an equation with one unknown, h. Some obvious bounds can be placed on h. In units of radians, $0 \le r_i \le \pi$. Since this must hold for every r_i, it follows that

$$h_{\min} = -\min_i k_i \le h \le \pi^2 - \max_i k_i = h_{\max}$$

. Within these bounds, there may be at most two solutions for h. In most applications, the solution with smaller h, nearer to the control triangle, is the desirable one. Let $\mathbf{A} = \left(\mathbf{V}^\top \mathbf{V}\right)^{-1}$, where $\mathbf{A}$ is symmetric and positive semi-definite, and $f(h) = \mathbf{c}^\top \mathbf{A}\mathbf{c} - 1$. See Figure 2 for a plot of $f(h)$ for various points. The derivative of $f(h)$ is

$$f'(h) = -\mathbf{c}^\top \mathbf{A}\mathbf{b} \tag{15}$$

where $\mathbf{b}$ is the vector with ith component $\operatorname{sinc}\left(\sqrt{k_i + h}\right)$, and the function $\operatorname{sinc}(x)$ is defined as so:

$$\operatorname{sinc}(x) = \begin{cases} 1 & \text{if } x = 0, \\ \frac{\sin x}{x} & \text{otherwise.} \end{cases} \tag{16}$$

Note that $f'(h)$ and $f(h)$ share many of the same terms, making the calculation more efficient. If needed for numerical purposes, the compositions of trig functions with square root can be smoothly extended to negative values: when $x < 0$, $\cos\sqrt{x} = \cosh\sqrt{-x}$ and $\frac{\sin\sqrt{x}}{\sqrt{x}} = \frac{\sinh\sqrt{-x}}{\sqrt{-x}}$.

Given all the preceding, Newton's method can be applied to solve for h. Using $h_{\min}$ as an initial guess, a good approximation is achieved for points inside the control triangle within only a few iterations. Better initial guesses are possible, but don't appear to be worth the cost of calculation. Convergence is somewhat slower further away from the control triangle, and is worst at the boundary of the projection. This is expected: at the boundary, the function reaches a minimum at the same place as its root, $f(h) = f'(h) = 0$, and Newton's method converges at a merely linear rate.[1]

3.2. **Without spherical approximation.** The method for spheres is not extensible to ellipsoids. Geodesic circles cannot in general be described as the intersection of a plane and a surface. Also, we can no longer make the assumption that the Euclidean norm $\|\mathbf{v}\|$ is constant. In general, these sort of problems are harder on an ellipsoid than a sphere. Geodesic circles are usually calculated in most software by brute force: extending a number of lines from a center point and using the endpoints as an approximation of the circle.[**?**] It is not surprising that an analytic form, or form with an easy numerical iteration, is not available here.

The spherical approximation is reasonably close to an ellipsoidal calculation. Figure 3 demonstrates the results of performing the forward transformation with the ellipsoid and then transforming it back using the spherical inverse transformation, and then calculating the deviation in distance of each point. Within the control triangle, the deviation does not exceed 25 kilometers, and within the hemisphere containing the control triangle, no more than 60 near the south pole.

4. Comparison

For comparison purposes, we use a control triangle with vertices at 22°N 0°E, 22°N 45°E, and 22°S 22.5°E, covering Africa. These coordinates are used for demonstrations of the Chamberlin trimetric projection in several places online,

To measure distortion of area and angle, this section uses the areal scale factor s and maximum angular deformation ω as defined in equations 12-15, 27, and 28 in section 4 of Snyder.[5] Derivatives are estimated numerically from a 1-degree grid.

FIGURE 4. Areal scale factor s. Left is Chamberlin, right is Linear.

FIGURE 5. Maximum angular deformation ω. Left is Chamberlin, right is Linear.

FIGURE 6. Distance deviation. Left is Chamberlin, right is Linear.

FIGURE 7. Distance difference between Chamberlin and Linear.

There is not a standard measurement of distance distortion for map projections, as map projections that do preserve distance can only do so along a finite number of geodesics.

4.1. **Extremal cases.** With both projections, points within or near the antipodal triangle may be projected so that they overlap points near or within the control triangle. Such points can be determined by the areal scale factor: points with positive scale factor lie in the usual range of the projection, while those with negative scale factor will overlap, and those where the scale factor is 0 lie on the boundary. The overlap is projected in the reverse orientation.

For the control triangle used in this text, the overlap area is part of the Pacific Ocean, as depicted in Figure 8. For the Chamberlin projection, the area is a rounded triangle surrounding the antipodal triangle, while for the projection introduced in this text, it is a three-lobed shape where two lobes meet at each vertex of the antipodal triangle.

Figure 9 shows the projection of the whole globe, including the overlap. In the Chamberlin projection, the boundary of the overlap is roughly elliptical. The boundary of the projection presented here instead has the form of a rounded triangle. In general the islands contained in this area are too small to be visible in projection, but the Hawaiian islands, which are near the northernmost vertex, do appear. On the Chamberlin projection, they are highly distorted. On the other projection, one can see that they are reversed. For large control triangles approaching a hemisphere, the boundary approaches a triangle with straight edges (not pictured).

5. Conclusion

We have to admit that a certain amount of complexity is hidden in the geodetic distance $d(\mathbf{v}_a, \mathbf{v}_b)$: on an ellipsoid, calculating geodetic distance is normally done using Vincenty's formula, which is an iterative method, or a descendent.[4] Of course, the Chamberlin projection uses the same calculation, so this is not a strike against the projection presented here, but it would be misleading to describe this projection as only consisting of a matrix transformation.

As this projection is a compromise projection that does not perfectly preserve area, angle, or distance, it is no large sin in this case to use the spherical approximation, in which the geodetic distance is simple trigonometry. We also note that the inverse transformation formula on the sphere, which uses a Newton's method iteration, is no more complicated than the inverse transformation for the Snyder equal area projection. [6]

The form of the forward formula suggests a possible family of projections that are simple functions of r_i, such as a polynomial function. (elaborate)

The Chamberlin projection is only applicable to surfaces of nonnegative curvature (or comparable non-differentiable surfaces), since the circles in the target plane must overlap. The projection presented here gives a result for all possible values of r_i, regardless of the relationship among them due to the underlying surface. It follows that this projection can be applied to any surface possessing a metric: hyperbolic surfaces, tori, and so on.

References

[1] R.L. Burden and J.D. Faires. Solutions of equations in one variable. In *Numerical Analysis*, pages 67–85. Cengage Learning, 2010.

FIGURE 8. Antipodal area. Solid line is Linear, dashed line is Chamberlin. The small triangles inside the dashed line are numerical error.

FIGURE 9. Projection of entire globe. Left: Chamberlin, Right: Linear.

[2] Albert H.J. Christensen. The chamberlin trimetric projection. *Cartography and Geographic Information Systems*, 19(2):88–100, 1992.
[3] A.S. Posamentier and C.T. Salkind. *Challenging Problems in Geometry*. Dover Books on Mathematics. Dover Publications, 2012.
[4] PROJ contributors. *PROJ coordinate transformation software library*. Open Source Geospatial Foundation, 2019.
[5] John P Snyder. *Map projections–A working manual*, volume 1395. US Government Printing Office, 1987.
[6] John P Snyder. An equal-area map projection for polyhedral globes. *Cartographica: The International Journal for Geographic Information and Geovisualization*, 29(1):10–21, 1992.
[7] John Parr Snyder and Philip M Voxland. *An album of map projections*. Number 1453. US Government Printing Office, 1989.
[8] G. Strang. *Linear Algebra and Its Applications*. Academic Press, 1980.
[9] M. Wohlgemuth. *Mathematisch für fortgeschrittene Anfänger: Weitere beliebte Beiträge von Matroids Matheplanet*. Spektrum Akademischer Verlag, 2010.